J. Fluid Mech. (1977), *vol.* 82, *part* 2, *pp.* 289–307
Printed in Great Britain

Stress in a suspension near rigid boundaries

By AYDIN TÖZEREN AND RICHARD SKALAK

Department of Civil Engineering and Engineering Mechanics, Columbia University, New York 10027

(Received 13 June 1975 and in revised form 3 May 1976)

The stress system near a rigid boundary in a suspension of neutrally buoyant spheres is considered under the assumption of small Reynolds number. The suspending fluid is assumed to be Newtonian and incompressible. An ergodic principle is formulated for parallel mean flows, and the bulk stress is expressed as a surface average. Only dilute suspensions are considered and particle interactions are neglected. A uniform shear flow past a plane wall with a single spherical particle is studied first. A series solution is developed and the mean velocity and stress fields are computed for a force-free and couple-free sphere and also for spheres with couples applied by external means. The translational and angular velocities of the particle and the stress distribution on the surface of the particle are calculated. Properties of dilute suspensions of spheres are found by appropriate surface averages over the solutions for a single particle. The mean stress on a plane parallel to the wall is shown to reduce to the Einstein value when the distance from the boundary is sufficiently large. Mean velocity profiles of the suspension for Couette flow and Poiseuille flow are developed. It is shown that in an average sense particles rotate more slowly than the ambient fluid in a region approximately three sphere radii thick adjacent to the plane wall. But for the suspension as a whole, an apparent slip velocity always develops in this region. This results in an apparent viscosity which is less than the infinite-suspension value of Einstein.

1. Introduction

The theoretical literature on suspension flows is an extensive body of work dealing mainly with bulk properties of suspensions. Starting with Einstein's (1906) work on a dilute suspension of rigid spheres, solutions of the Navier–Stokes equations for the flow due to the presence of one or more particles have been used to derive the relation of the bulk or mean stress in a suspension to the mean velocity gradient. Recent studies of general suspension properties have been given by Batchelor (1970, 1973), Cox & Brenner (1971) and Brenner (1972*a*, *b*). Further developments have included the study of more concentrated suspensions (Batchelor & Green 1972), deformable and non-spherical particles (Roscoe 1967; Batchelor 1971; Hinch 1972; Brenner 1972*b*) and the effects of Brownian motion (Brenner 1972*a*; Leal & Hinch 1972; Hinch & Leal 1972; Brenner & Weissman 1972). In most of these developments, the suspension has been assumed to be dilute and the scale of the macroscopic flow to be large compared with the particle spacing. Specifically, let a represent a typical dimension of the particle, let l be the average distance between particles and let R_0 characterize the scale of gradients of the bulk quantities (including concentration) or the typical

length scale of the boundaries of the flow (e.g. the tube radius). Then it is usually assumed that

$$a/R_0 \ll a/l \ll 1. \tag{1.1}$$

In the presence of a boundary, the bulk properties of the suspension are not applicable in a thin layer near the boundary, of the order of a few particle radii in thickness. The aim of the present paper is to examine the structure of this wall layer. Only dilute suspensions are considered and the inequalities (1.1) are assumed to hold for the suspension as a whole excluding the wall layer. Within the wall layer, the gradients of the mean velocity and particle concentration vary on a scale comparable to the particle size. Consequently, although ensemble averages are well defined in the wall region, an ergodic principle equating volume averages to ensemble averages is no longer valid. In the present study ensemble averages in the wall region are equated to areal averages over surfaces parallel to the wall. The basic assumption made is that there exist surfaces, parallel to the wall, over which the dependent flow variables are statistically uniform and have average values which are functions only of the distance from the wall. This rationale is elaborated further in the next section.

The problem of wall effects in suspension rheology has a considerable history, but most theoretical treatments which consider more than one particle at a time are based on approximate models. For example, in regard to flow of suspensions through circular tubes, the flow is typically divided into a wall layer assumed to contain suspending fluid only and a core region with uniform bulk suspension properties (Maude & Whitmore 1956; Whitmore 1959; Maude 1967). This model can reproduce experimental data on the apparent viscosity of the suspension by suitable adjustment of the wall-layer thickness. But the velocity distribution predicted in the wall region cannot be accurate since particles may intrude into it. Further, the motions of the particles themselves are not accurately described.

Cox & Brenner (1971) have considered the wall effects starting from basic solutions for a single particle, but have truncated series in powers of a/l. The present paper supplies detailed information supporting their conclusion that the wall layer will generally result in an apparent slip of the bulk suspension relative to the wall.

The study of the flow of a suspension past a rigid wall may be posed as two separate problems which ideally should be solved sequentially. The first is (*a*) given some initial distribution of particles and appropriate boundary conditions far from the wall, find the velocity and stress fields. The second is (*b*) starting from the given particle distribution (*a*) find the time history of the subsequent particle distribution. In the present paper only problem (*a*) is addressed. In principle, if sufficient cases (*a*) are solved, integration over the velocity fields may be used to solve (*b*). In the present paper, problem (*b*) is not solved because it requires a study of collisions of particles near a wall, which have been neglected. Such interactions of particles near the wall are important to (*b*) but not to (*a*) assuming that only a small percentage of the particles are involved in collisions at a given time when the particle concentration is small.

One purpose of the present study is to provide a basis for the evaluation of continuum theories which purport to represent a suspension both in regard to its mean velocity distribution and the particle rotations, such as microstructure theories (see reviews by Ariman, Turk & Sylvester 1973, 1974; Cowin 1974). In these theories the wall layer is hopefully reproduced in considerable detail, but appropriate boundary conditions are still problematical.

The present study employs integration over solutions for a single sphere in a shear flow past a plane rigid wall. It may be shown that this is a correct procedure to order c, where c is the volumetric concentration (Tözeren 1974). Various problems for single spheres have previously been studied both theoretically and experimentally. Solutions for a rotating sphere and for a translating sphere in a viscous fluid near a plane wall were given by Dean & O'Neill (1963) and O'Neill (1964) respectively. The translational and angular velocities of a neutrally buoyant sphere near a plane wall were derived by Goldman, Cox & Brenner (1967). These solutions are extended and incorporated below.

2. Balance laws governing suspensions

A suspension is regarded as a system which is determinate only in a statistical sense. It is expected that the exact location of the particles will be different for different realizations of a suspension under the same macroscopic conditions, i.e. with the same shape and motion of the boundaries of the suspension. However, as shown by Batchelor (1970), taking ensemble averages of the equations of continuity and motion yields the governing equations for the mean flow:

$$\partial U_i/\partial x_i = 0 \tag{2.1}$$

and

$$\frac{\partial}{\partial x_j}\Sigma_{ij} + \bar{f}_i = \rho\left(\frac{\partial U_i}{\partial t} + U_j\frac{\partial U_i}{\partial x_i}\right), \tag{2.2}$$

where Σ_{ij} is the bulk stress, defined as

$$\Sigma_{ij} + \bar{\sigma}_{ij} - \rho\overline{(u_i - U_i)(u_j - U_j)}. \tag{2.3}$$

In these equations u_i is the velocity in any one realization, U_i is the ensemble average of u_i, σ_{ij} and f_i are the stress tensor and body force in any realization and an overbar indicates an ensemble average. Since only slow viscous flow of the suspension will be considered, the inertial terms $\rho\overline{(u_i - U_i)(u_j - U_j)}$ in (2.3) will be neglected.

The ensemble average of any quantity is assumed, as in Batchelor (1970), to be equal to the average of the same quantity in any particular realization over any line, surface or volume with respect to which this quantity is statistically stationary. Far from rigid boundaries, volume averages are most often used.

In the wall region, gradients normal to the wall are of the order of the particle size and ensemble averages cannot be replaced by volume averages. However, where the flow in the wall layer is essentially parallel to the wall and gradients along the wall are small or zero, we may expect that there exist surfaces parallel to the wall, with dimensions large compared with l, over which the suspension properties are statistically uniform. Under these conditions, averages of the flow properties over these surfaces will be equal to the ensemble averages. Such averages will be functions of the distance, say x_2, from the wall.

For example, the particle concentration c is defined in terms of ensemble averages at any point $(\mathbf{x}, t)$ as the ratio of the number of realizations in which this point is occupied by a solid particle to the total number of realizations. The equivalent areal average is

$$c(x_2) = A^*/A,$$

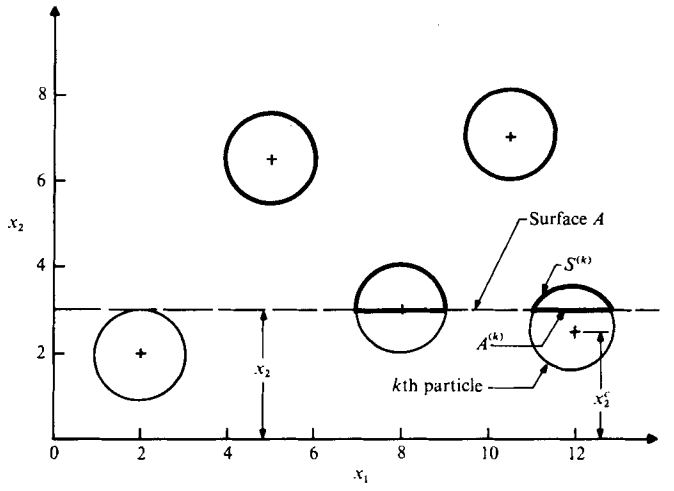

FIGURE 1. Schematic representation of a suspension. Areal averages are taken over the surface A for parallel flows.

where A^* is the area of all the particles cut by the surface and A is the total area of the surface, i.e.

$$A^* = \sum_{k=1}^{R} A^{(k)},$$

where $A^{(k)}$ is the area of intersection of the kth particle with the surface $x_2 =$ constant and R is the total number of particles intersecting the surface (see figure 1).

Assuming the rigid boundary to be $x_2 = 0$ and the mean velocity to be in the x_1 direction, the component of the bulk stress of interest is Σ_{12}. Expressed as an areal average it is

$$\Sigma_{12} = \frac{1}{A}\int_{A-A^*} 2\mu e_{12}\, dA + \frac{1}{A}\int_{A^*} \sigma_{12}\, dA, \tag{2.4}$$

where e_{12} is the instantaneous strain-rate component in any realization and σ_{12} is the stress component within the solid particles. For uniform particles, the stress and strain fields within the particles may be taken to be the limiting values for elastic spheres as the elastic moduli of the spheres approach infinity. (For non-uniform or hollow rigid spheres it may be shown that the motion of the particles and fluid are the same as for uniform rigid spheres provided the centre of mass is at the centre of each sphere.) Since the strain rate is identically zero within the rigid particles, (2.4) may be written as

$$\Sigma_{12} = 2\mu E_{12} + \frac{1}{A}\int_{A^*} \sigma_{12}\, dA, \tag{2.5}$$

where E_{ij} is the bulk strain-rate tensor $\frac{1}{2}(U_{i,j} + U_{j,i})$. The last term in (2.5) is called the particle stress $\Sigma_{12}^{(p)}$. Since the particles in the suspension are assumed to be free of body forces, $\Sigma_{12}^{(p)}$ can be computed from the stresses on the surface of the particle, i.e.

$$\Sigma_{12}^{(p)} = \frac{1}{A}\sum_{k=1}^{R}\int_{A^{(k)}} \sigma_{12}\, dA = \frac{1}{A}\sum_{k=1}^{R}\int_{S^{(k)}} \sigma_{ij} n_j\, dA, \tag{2.6}$$

where $S^{(k)}$ denotes the portion of the surface of the kth particle that remains above the surface A as shown in figure 1. The last term in (2.6) avoids the need to consider the internal stress distribution in the particles any further.

3. Slow viscous shear flow containing a sphere near a plane wall

Consider steady slow viscous motion of an incompressible liquid which is bounded by an infinite plane, has a simple shearing motion and contains a solid force-free sphere at an arbitrary distance from the plane wall. The equations governing the motion of the fluid are

$$\partial p/\partial x_i = \mu\, \partial^2 u_i/\partial x_j^2, \tag{3.1}$$

$$\partial u_i/\partial x_i = 0, \tag{3.2}$$

where p is the fluid pressure and μ is the viscosity of the fluid. Let $x_2 = 0$ be the bounding plane and assume that the fluid motion is in the x_1 direction. The co-ordinates x_i, from here on, are made dimensionless by the sphere radius a. The centre of the sphere is located at $(0, d/a, 0)$.

When the fluid is at rest at infinity, solutions for the motion of the fluid when the sphere either translates parallel to the wall or rotates about an axis parallel to x_3 were obtained by O'Neill (1964) and Dean & O'Neill (1963) respectively.

For the problem considered here it is convenient to superpose three solutions. Let $\mathbf{u}_T$ be the velocity field of the fluid when the sphere translates with unit velocity and let $\mathbf{u}_R$ denote the velocity field when the sphere rotates with unit angular velocity. Further, let $\mathbf{u}_S$ be the solution when the sphere is fixed in a fluid whose motion in the absence of the sphere would be the simple shear flow at a shear rate S. Then the solution of the proposed problem of a force-free sphere may be written as

$$\mathbf{u} = U\mathbf{u}_T + \Omega\mathbf{u}_R + \mathbf{u}_S, \tag{3.3}$$

where U and Ω are the translational and rotational velocities of the sphere, which are to be determined by setting the resultant force acting on the sphere to zero and equating the sum of the external couple and the couple due to the fluid to zero.

It was shown by Goldman *et al.* (1967) that the resultant force and couple acting on the sphere for the solution $\mathbf{u}_S$ can be obtained, by a suitable quadrature scheme, from the corresponding quantities when the sphere either translates or rotates uniformly in a fluid at rest. While this allows computation of U and Ω it does not yield the complete velocity and stress fields. Hence the detailed solution $\mathbf{u}_S$ is calculated by a method of separation of variables similar to that of Dean & O'Neill (1963).

A solution for the velocity field $\mathbf{u}_S$ and pressure p in cylindrical co-ordinates (ar, θ, az) may be developed in the form

$$a^2 p = \mu S Q_1 \cos\theta, \tag{3.4}$$

$$u = \tfrac{1}{2} aS\,(rQ_1 + k(U_0 + U_2) + 2z)\cos\theta, \tag{3.5}$$

$$v = \tfrac{1}{2} aS\,(k(U_2 - U_0) - 2z)\sin\theta, \tag{3.6}$$

$$w = \tfrac{1}{2} aS\,(zQ_1 + 2kw_1)\cos\theta, \tag{3.7}$$

where Q_1, U_0, U_2 and w_1 are functions of r and z only. The bounding plane is $z = 0$ and the z axis is chosen to pass through the centre of the sphere.

It is convenient to introduce bispherical co-ordinates (ξ, η) defined by

$$r = \frac{k \sin \eta}{\cosh \xi - \cos \eta}, \quad z = \frac{k \sinh \xi}{\cosh \xi - \cos \eta} \quad (0 \leqslant \eta \leqslant \pi). \tag{3.8}$$

The constant k is determined by choosing the plane $z = 0$ to be $\xi = 0$ and the surface of the sphere to be $\xi = \alpha > 0$, so that

$$1 = k \operatorname{cosech} \alpha, \quad d/a = k \coth \alpha. \tag{3.9}$$

The equations for w_1, Q_1, U_0 and U_2 were shown by Jeffery (1915) to be of the form

$$w_1 = (\cosh \xi - \bar{\mu})^{\frac{1}{2}} \sin \eta \sum_{n=1}^{\infty} [A_n \sinh (n+\tfrac{1}{2}) \xi] P_n'(\bar{\mu}), \tag{3.10}$$

$$Q_1 = (\cosh \xi - \bar{\mu})^{\frac{1}{2}} \sin \eta \sum_{n=1}^{\infty} [B_n \cosh (n+\tfrac{1}{2}) \xi + C_n \sinh (n+\tfrac{1}{2}) \xi] P_n'(\bar{\mu}), \tag{3.11}$$

$$U_0 = (\cosh \xi - \bar{\mu})^{\frac{1}{2}} \sum_{n=0}^{\infty} [D_n \cosh (n+\tfrac{1}{2}) \xi + E_n \sinh (n+\tfrac{1}{2}) \xi] P_n(\bar{\mu}), \tag{3.12}$$

$$U_2 = (\cosh \xi - \bar{\mu})^{\frac{1}{2}} \sin^2 \eta \sum_{n=2}^{\infty} [F_n \cosh (n+\tfrac{1}{2}) \xi + G_n \sinh (n+\tfrac{1}{2}) \xi] P_n''(\bar{\mu}), \tag{3.13}$$

where $\bar{\mu}$ denotes $\cos \eta$ and $P_n(\bar{\mu})$ is the Legendre polynomial of order n. The primes indicate differentiations with respect to $\bar{\mu}$.

The coefficients A_n, B_n, C_n, D_n, E_n, F_n and G_n are determined by boundary conditions and the equation of continuity. The velocity must be zero on the bounding plane $z = 0$ and from the equation of continuity it follows that $\partial w/\partial z = 0$ also on $z = 0$. These conditions require that (Dean & O'Neill 1963)

$$B_n = (n-1) A_{n-1} - (2n+1) A_n + (n+2) A_{n+1} \quad (n \geqslant 1), \tag{3.14}$$

$$D_n = -\tfrac{1}{2}(n-1) n A_{n-1} + \tfrac{1}{2}(n+1)(n+2) A_{n+1} \quad (n \geqslant 0), \tag{3.15}$$

$$F_n = \tfrac{1}{2}(A_{n-1} - A_{n+1}) \quad (n \geqslant 2). \tag{3.16}$$

Since the sphere is fixed in the shear flow, the velocity must be zero on the surface of the sphere and must approach the undisturbed shear velocity $z \to \infty$. These conditions require (Tözeren 1974)

$$C_n = -2k_n \left[\frac{(n-1) A_{n-1}}{2n-1} - A_n + \frac{(n+2) A_{n+1}}{2n+3} \right] \quad (n \geqslant 1), \tag{3.17}$$

$$E_n = -2^{\frac{3}{2}} \operatorname{cosech} [(n+\tfrac{1}{2}) \alpha] (2n+1) \exp [-(n+\tfrac{1}{2}) \alpha] + k_n \left[\frac{(n-1) n A_{n-1}}{2n-1} - \frac{(n+1)(n+2) A_{n+1}}{2n+3} \right] \quad (n \geqslant 0), \tag{3.18}$$

$$G_n = -k_n \left[\frac{A_{n-1}}{2n-1} - \frac{A_{n+1}}{2n+3} \right], \tag{3.19}$$

where

$$k_n = (n+\tfrac{1}{2}) \coth [(n+\tfrac{1}{2}) \alpha] - \coth \alpha \quad (n \geqslant 0). \tag{3.20}$$

Now the equation of continuity can be used to derive a system of equations for the constants A_n:

$$[(2n-1)k_{n-1}-(2n-3)k_n]\left[\frac{(n-1)A_{n-1}}{2n-1}-\frac{nA_n}{2n+1}\right]$$
$$-[(2n+5)k_n-(2n+3)k_{n+1}]\left[\frac{(n+1)A_n}{2n+1}-\frac{(n+2)A_{n+1}}{2n+3}\right]$$
$$=2^{\frac{1}{2}}\operatorname{cosech}[(n-\tfrac{1}{2})\alpha](2n-1)\exp[-(n-\tfrac{1}{2})\alpha]-2^{\frac{3}{2}}\operatorname{cosech}[(n+\tfrac{1}{2})\alpha](2n+1)$$
$$\times\exp[-(n+\tfrac{1}{2})\alpha]+2^{\frac{1}{2}}\operatorname{cosech}[(n+\tfrac{3}{2})\alpha](2n+3)\exp[-(n+\tfrac{3}{2})\alpha]. \quad (3.21)$$

The first r equations in the set (3.21) contain the $r+1$ constants $A_1, A_2, \ldots, A_{r+1}$, and determine $A_1, \ldots, A_r$ if A_{r+1} is assumed to be zero. The equations are solved on this assumption for increasing r until convergence to $0{\cdot}001A_1$ is obtained. The number r of equations required for convergence of the solution increases as the value of α decreases.

For purposes of calculating the particle stress, it is necessary to compute the total force acting on the part $S^{(k)}$ of the surface of the sphere remaining above an arbitrary plane z = constant. Let this force be T_{1S} for a fixed sphere in a shear flow S. It is found that

$$T_{1S}=\int_{S^{(k)}}\sigma_{ij}n_j\,dS=-\pi\mu k^2a^2\frac{S}{2}\left[\int_t^1\frac{\partial Q_1}{\partial\xi}\frac{\sin\eta\,d\bar{\mu}}{(\cosh\alpha-\bar{\mu})^2}\right.$$
$$+2\int_t^1\frac{\partial U_0}{\partial\xi}\frac{d\bar{\mu}}{(\cosh\alpha-\bar{\mu})}+\sinh\alpha\int_t^1\frac{Q_1\sin\eta\,d\bar{\mu}}{(\cosh\alpha-\bar{\mu})^3}$$
$$\left.+\frac{1}{k^2}\frac{2(z-d)^2-2a^2}{a^2}\right], \quad (3.22)$$

where

$$t=\frac{d}{a}-\left[\left(\frac{d}{a}\right)^2-1\right]\Big/\frac{z}{a}. \quad (3.23)$$

This expression for the force acting on the part $S^{(k)}$ of the surface of the sphere is similar to those obtained for a complete sphere rotating (Dean & O'Neill 1963) and translating (O'Neill 1964). For these cases, the same series expansions may be used, subject to the appropriate boundary conditions. To modify (3.23) to apply to the case of a sphere translating in fluid at rest at infinity, the k^2S in front of the square bracket is replaced by kU, and the last term in the square bracket is dropped. In the case of a sphere rotating in a fluid at rest, the constant k^2S is replaced by $k^2\Omega$ and the last term in the square bracket is divided by -2.

Returning to the complete problem of a force-free sphere subject to an external couple M_3 in a semi-infinite shear flow, the translational and angular velocities of the sphere are found by setting the resultant force equal to zero and the resultant couple equal to $-M_3$, i.e.

$$F_S+F_T\,U+F_R\,\Omega=0, \quad (3.24)$$

$$M_S+M_T\,U+M_R\,\Omega+M_3=0, \quad (3.25)$$

where M_S, M_T and M_R are the resultant couples in each solution. Equation (3.24) may be reduced to

$$S\sum_{n=0}^{\infty}E_n^{(S)}+\Omega\sum_{n=0}^{\infty}E_n^{(R)}+\frac{U}{k}\sum_{n=0}^{\infty}E_n^{(T)}=0, \quad (3.26)$$

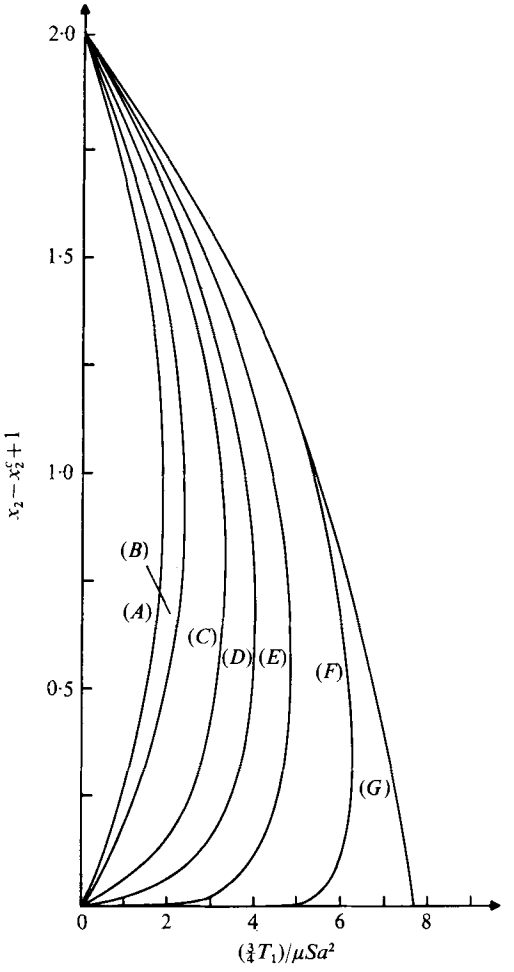

FIGURE 2. Force T_1 on a portion of a particle as a function of the location of the cutting plane A (figure 1). Each curve is for a sphere with centre at a different distance x_2^c from the boundary.

Curve	(A)	(B)	(C)	(D)	(E)	(F)	(G)
x_2^c	3·5	1·5	1·05	1·01	1·001	$1+10^{-8}$	1·0

where the superscripts S, R and T identify the coefficients for the solutions $\mathbf{u}_S$, $\mathbf{u}_R$ and $\mathbf{u}_T$. Equation (3.25) for the total couple acting on the force-free sphere similarly reduces to

$$M_3 = 2\tfrac{2}{3}\pi\mu\frac{U}{k}a^2\sinh^2\alpha\sum_{n=0}^{\infty}[2n(n+1)A_n^{(T)}] + 2\tfrac{2}{3}\pi\mu\Omega a^3\sinh^3\alpha\sum_{n=0}^{\infty}[2n(n+1)A_n^{(R)}] + 2\tfrac{2}{3}\pi\mu Sa^3\sinh^3\alpha\sum_{n=0}^{\infty}[2n(n+1)A_n^{(S)}]. \tag{3.27}$$

The coefficients $A_n^{(S)}$ and $E_n^{(S)}$ are the A_n and E_n determined by (3.21) and (3.18) for a fixed sphere in a shear flow as discussed above. The coefficients $A_n^{(R)}$, $E_n^{(R)}$, $A_n^{(T)}$ and $E_n^{(T)}$ for translation and rotation of the sphere may be found from equations given by Dean & O'Neill (1963) and O'Neill (1964) or Tözeren (1974).

In computations for particular cases, the $A_n^{(S)}$, $A_n^{(R)}$ and $A_n^{(T)}$ are computed first and they determine $E_n^{(S)}$, $E_n^{(R)}$ and $E_n^{(T)}$. Next, U/kS and Ω/S are obtained by solving (3.24) and (3.25). Finally, the force $T_1(x_2, x_2^c)$ acting on a segment of the sphere is computed by evaluating (3.22) numerically (x_2^c is the sphere centre, i.e. $x_2^c = d/a$).

Values of $T_1/\mu S a^2$ for several values of x_2^c are plotted as a function of $x_2 - x_2^c + 1$ in figure 2 for the case where the couple M_3 is zero. It is seen that when x_2^c is large T_1 is symmetric with respect to $x_2 - x_2^c$ as expected. As the sphere approaches the wall, the distribution of stress becomes increasingly asymmetric. Ultimately, a point force develops at the point of contact of the sphere and the wall in the limit $x_2^c \to 1$ (O'Neill 1968).

The series solutions outlined above converge poorly in the numerical sense as the ratio of the gap width δ to the sphere radius tends to zero. They are, in fact, computationally useless for δ/a less than about 0·01. Asymptotic methods in this range were developed by Goldman *et al.* (1967) and their solutions have been adapted to cover this range approximately (see Tözeren 1974). Fortunately, very few spheres fall into this range and their influence is not important to the final results.

4. Particle stress and effective viscosity

To compute the particle stress [see (2.6)] using the solutions for a single particle, it is necessary to integrate over all the intersections of particles at various distances from the wall with the plane x_2 = constant. The force for any one particle intersection is $T_1(x_2, x_2^c, E_{12}, M_3)$, where x_2 is the location of the section, x_2^c is the centre of the sphere, E_{12} is the mean strain rate and M_3 is the external couple applied to the particle. Let $h(x_2^c)$ be the average number density per unit area of the particles whose centres are at x_2^c. Then (2.6) is equivalent to

$$\Sigma_{12}^{(p)} = \int_{x_2^*}^{x_2+1} h(x_2^c)\, T_1(x_2, x_2^c, M_3, E_{12})\, dx_2^c, \tag{4.1}$$

where the lower limit of integration x_2^* is given by

$$x_2^* = \begin{cases} 1 & \text{if} \quad x_2 < 2, \qquad (4.2) \\ x_2 - 1 & \text{otherwise.} \qquad (4.3) \end{cases}$$

The number density $h(x_2^c)$ is such that the number of sphere centres in a volume extending from x_2 to $x_2 + \Delta x_2$ with unit cross-sectional area parallel to x_2 = constant is

$$n(x_2, \Delta x_2) = \int_{x_2}^{x_2+\Delta x_2} h(x_2^c)\, dx_2^c. \tag{4.4}$$

It is easy to see from the solutions given above that $\Sigma_{12}^{(p)}$ is linear in E_{12}, μ and c^0, where c^0 is the uniform concentration far from the wall. It is convenient to extract these from (4.1) and define a function $f(x_2, h, m)$ such that

$$\Sigma_{12}^{(p)} = 2\mu c^0 E_{12} f(x_2, h, m), \tag{4.5}$$

where $m = M_3/\mu E_{12} V_0$ and V_0 is the volume of one particle. At the wall $f = 0$ because the area A^* over which $\Sigma_{12}^{(p)}$ is integrated approaches zero. The function f is known far from the wall from the previous literature for an infinite suspension:

$$\lim_{x_2 \to \infty} f(x_2) = f^\infty = 2{\cdot}5 + M_3/4\mu E_{12} V_0, \tag{4.6}$$

where the term 2·5 is due to Einstein (1906) and the second term was given by Brenner (1972*a*) for infinite shear flow. In terms of the particle rotation (4.6) becomes

$$f^{\infty} = 2{\cdot}5 + (1{\cdot}5\Omega^{\infty}/E_{12} + 1{\cdot}5), \tag{4.7}$$

where Ω^{∞} is the mean particle rotation far from the wall. The asymptotic values of f provide a check on the computations. Agreement with the asymptotic values was found to be within 1 % for all of the cases computed. (See the next section.)

The function $f(x_2)$ may be interpreted as the intrinsic increase in apparent viscosity due to the presence of the particles. From (2.5) and (4.5), the total bulk stress is

$$\Sigma_{12} = 2\mu E_{12}[1 + c^0 f(x_2)]. \tag{4.8}$$

In this case it is convenient to define the effective viscosity μ_e by

$$\mu_e = \Sigma_{12}/2E_{12} = \mu[1 + c^0 f(x_2)]. \tag{4.9}$$

Equation (4.9) may be used to compute the mean velocity profile by solving for E_{12} and integrating. To first order in c^0, the result is

$$U_1 = aS\left(x_2 + f^{\infty}c^0 x_2 - c^0\int_0^{x_2} f(x_2)\,dx_2\right), \tag{4.10}$$

where c^0 and S are the concentration and mean velocity gradient as $x_2 \to \infty$. In the shear flows considered here, the stress component Σ_{12} is constant and is greater than the stress which would occur in the suspending fluid alone at a shear rate S. At the wall the concentration c goes to zero and the full stress is carried by the fluid. This implies that, for the suspension, the strain rate E_{12} at the wall must be greater than its value at infinity ($E_{12}^{\infty} = \frac{1}{2}S$). This effect ensures that the velocity near the wall tends to increase more rapidly than in a uniform suspension and gives rise to a positive apparent slip velocity.

Next consider flow of a dilute suspension between two parallel plates a distance b apart due to the motion of the upper plate with velocity U_0 with the x_1 direction; $x_2 = 0$ denotes the lower plate and $x_2 = b/a$ is the upper plate. Assuming that (4.8) is valid in the vicinity of each plate with Σ_{12} equal to a constant, integration with respect to x_2 yields the first approximation in c^0:

$$U_1 = \frac{U_0 a}{b}\left\{x_2 + \frac{c^0 x_2 a}{b}\int_0^{b/a} f_1(x_2)\,dx_2 - c^0\int_0^{x_2} f_1(x_2)\,dx_2\right\}, \tag{4.11}$$

where

$$f_1(x_2) = \begin{cases} f(x_2) & \text{if} \quad x_2 < b/2a, \\ f(b/a - x_2) & \text{if} \quad x_2 > b/2a. \end{cases}$$

For this finite Couette flow it is also useful to introduce an apparent viscosity μ_a based only on macroscopic or global quantities. It is defined by

$$\mu_a = bT_0/U_0, \tag{4.12}$$

where $T_0 = \Sigma_{12}$. Using (4.8) and (4.11) in (4.12) gives

$$\mu_a = \mu\left(1 + c^0\frac{a}{b}\int_0^{b/a} f_1(x_2)\,dx_2\right). \tag{4.13}$$

In the case of flow in a circular pipe, it is assumed that

$$U_R = U_\theta = 0, \quad U_z = f(R), \tag{4.14}$$

$$\partial p/\partial z = G = \text{constant}, \tag{4.15}$$

where (R, θ, z) are cylindrical co-ordinates. For pipe flow, an ensemble average of any quantity at a position $\mathbf{x}$ is equal to the average over the cylindrical surface that passes through $\mathbf{x}$. But if the particle radius to pipe radius ratio $\lambda = a/R_0$ is sufficiently small the boundary surface can be approximated by a plane wall. It is shown by Bungay & Brenner (1969, 1973) that, when the pipe wall is replaced by a plane surface, the results are correct up to terms of first order in λ. Hence, for small λ, the particle stress component Σ_{Rz} is assumed to be to a first approximation

$$\Sigma_{Rz} = 2\mu\left[1 + c^0 f\left(\frac{R_0 - R}{a}\right)\right] E_{Rz}, \tag{4.16}$$

where R_0 is the radius of the pipe and x_2 is replaced by $(R_0 - R)/a$ in the expression for $f(x_2)$. E_{Rz} is the mean rate-of-strain component. Substituting (4.14)–(4.16) into the equations of motion and neglecting the higher-order terms in c^0, the velocity profile is found to be

$$U_z = \frac{G}{4\mu}(R_0^2 - R^2) - c^0 \frac{Ga^2}{2\mu}\int_0^{R'/a}\left(\frac{R_0}{a} - \frac{R'}{a}\right) f\left(\frac{R'}{a}\right) d\left(\frac{R'}{a}\right), \tag{4.17}$$

where R' is defined as $R_0 - R$. The apparent viscosity for pipe flow is defined as

$$\mu_a = \frac{\pi}{8}\frac{\partial p}{\partial z} R_0^4 Q^{-1}, \tag{4.18}$$

where $\partial p/\partial z$ is the pressure gradient in the z direction and Q is the discharge. Equation (4.18) is Poiseuille's law for a Newtonian fluid solved for the viscosity. If the discharge Q is calculated from (4.17), neglecting the higher terms in c^0, (4.18) reduces to

$$\mu_a = \mu\left[1 + c^0 \frac{8}{R_0^4}\int_0^{R_0} \frac{R^3}{2} f\left(\frac{R_0 - R}{a}\right) dR\right]. \tag{4.19}$$

Equation (4.19) shows that the apparent viscosity decreases with decreasing R_0/a as may be seen in the numerical examples in the next section.

5. Numerical examples

The expressions for the particle stress and the apparent viscosities derived in the previous section are general in that they apply to any particle distribution $h(x_2^c)$. This distribution is the result of entrance conditions, particle interactions and possibly Brownian motion and particle migration. This problem is not solved here, but to illustrate the possible results and for comparison with experimental data, several different distributions will be considered. These are shown in figure 3 (*B*). In all cases, $h = 0$ for $x_2^c < 1$, and far from the rigid boundary the concentration is assumed to be uniform and equal to c_0. In between the distributions assumed are as follows.

Case (*a*): $$h = 3c^0/4\pi a^2 \quad \text{for all} \quad x_2^c > 1. \tag{5.1a}$$

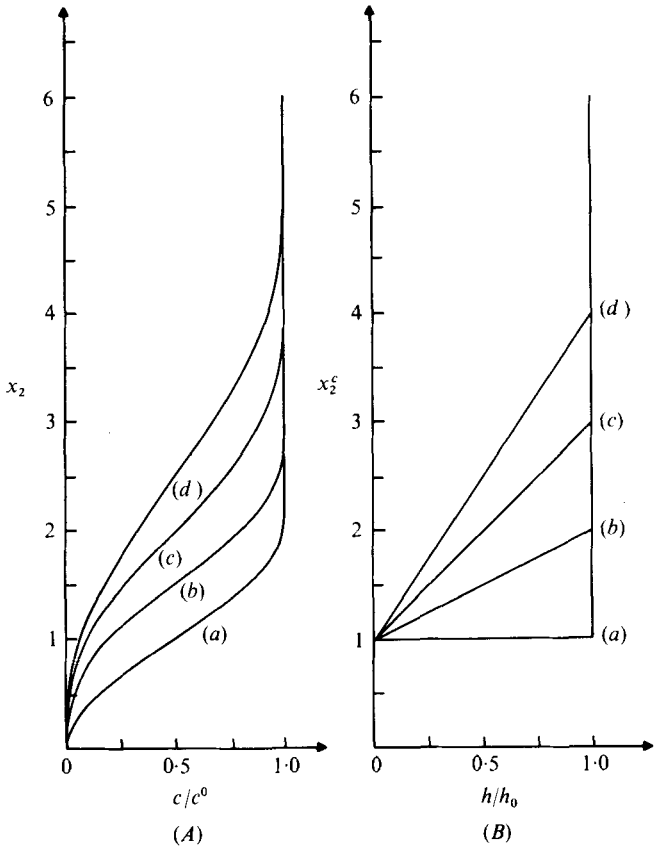

FIGURE 3. (*A*) Concentration c as a function of x_2 for the mean particle distributions $h(x_2^c)$ shown in (*B*). (*B*) The distributions $h(x_2^c)$ refer to the number density of particle centres.

$$\textit{Case (b)}: \qquad h = \begin{cases} (3c^0/4\pi a^2)\,(x_2^c - 1) & \text{if} \quad 1 < x_2^c < 2, \\ 3c^0/4\pi a^2 & \text{if} \quad x_2^c > 2. \end{cases} \tag{5.1b}$$

$$\textit{Case (c)}: \qquad h = \begin{cases} (3c^0/4\pi a^2)\,\tfrac{1}{2}(x_2^c - 1) & \text{if} \quad 1 < x_2^c < 3, \\ 3c^0/4\pi a^2 & \text{if} \quad x_2^c > 3. \end{cases} \tag{5.1c}$$

$$\textit{Case (d)}: \qquad h = \begin{cases} (3c^0/4\pi a^2) & \tfrac{1}{3}(x_2^c - 1) \quad \text{if} \quad 1 < x_2^c < 3, \\ 3c^0/4\pi a^2 & \text{if} \quad x_2^c > 4. \end{cases} \tag{5.1d}$$

Case (*a*) corresponds to a uniform distribution of centres outside the wall exclusion region.

The concentration on any plane x_2 is defined by (2.4) and is related to the distribution of centres $h(x_2^c)$ by

$$c = \int_{x_2^*}^{x_2+1} a^2 h(x_2^c)\,\pi[1 - (x_2^c - x_2)^2]\,dx_2^c, \tag{5.2}$$

where x_2^* is given by (4.2) and (4.3). The particle concentrations that result from the distributions $h(x_2^c)$ in figure 3(*B*) are shown in figure 3(*A*).

The function $f(x_2)$ defined in (4.5) was computed for force-free spheres for three values of the moment applied to each particle. The moments were chosen to give the

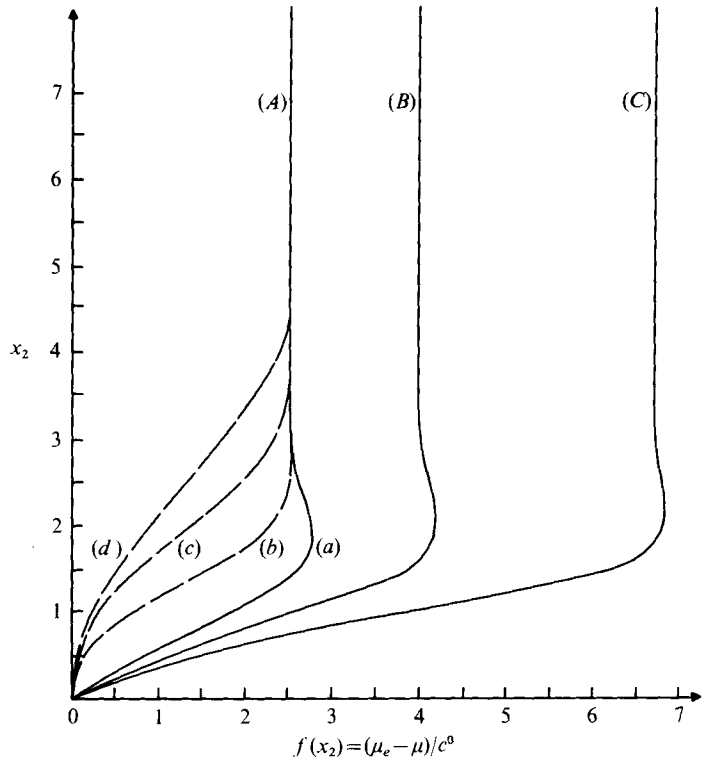

FIGURE 4. Increase in effective viscosity due to particle stress. (*A*) Suspension of neutrally buoyant particles ($\Omega = -\frac{1}{2}S$ as $x_2 \to \infty$). Curves (*Aa–d*) correspond to the concentration curves (*a*)–(*d*) in figure 3. (*B*) Suspension of particles with external couple ($\Omega = 0$ as $x_2 \to \infty$). (*C*) Suspension of particles with external couple ($\Omega = 0{\cdot}9S$ as $x_2 \to \infty$).

cases $\Omega^\infty = -\frac{1}{2}S$, 0 and $0{\cdot}9S$. The first of these corresponds to zero applied moment. The integral in (4.1) was evaluated numerically using values of T_1 at closely spaced points. The results are shown in figure 4. For the case of force-free and couple-free particles, the dependence of $f(x_2)$ on the mean particle distributions $h(x_2^c)$ in figure 3 is illustrated in figure 4 by curves (*a*), (*b*), (*c*) and (*d*). Curves (*Aa*), (*B*) and (*C*) are for uniform distributions of particle centres and different values of the external moment. In all cases, the function $f(x_2)$ approaches its asymptotic value within a distance of about $4a$ from the wall.

After the intrinsic viscosity functions $f(x_2)$ have been computed, the mean velocity may be computed using (4.10). The results are shown in figure 5 in terms of the difference of the mean velocity from a straight line for the same three applied moments as before with a uniform particle distribution (5.1*a*). The difference velocity shown in figure 5 approaches a constant far from the wall for each case. This constant is a positive apparent slip velocity of the bulk suspension relative to the wall in all cases. Figure 5 relates to the mean velocity of the entire suspension. It was found that the mean particle velocity near the boundary is also greater than $x_2 S$ in all cases, as shown in figure 6. The mean particle velocities shown are averages over the intersection A^* of a plane parallel to the boundary with the solid particles taking into account both the translation and the rotation of the particles. A similar average of

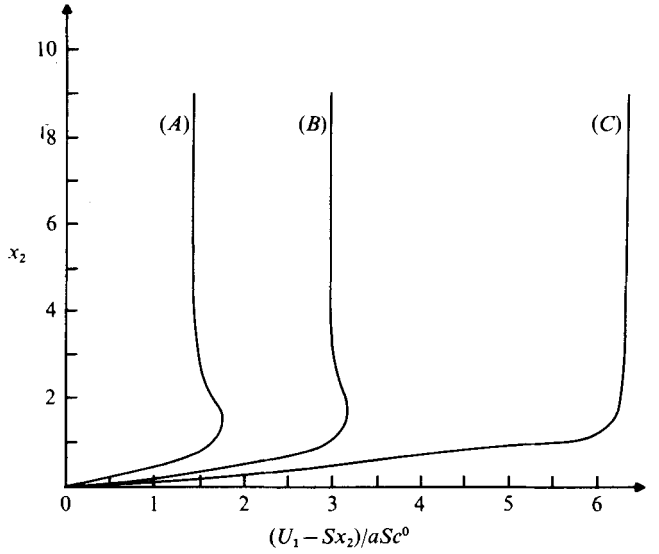

FIGURE 5. Mean velocity in a suspension in semi-infinite Couette flow. Curves (*A*), (*B*) and (*C*) correspond to three different moments applied to the particles giving $\Omega^\infty = -\frac{1}{2}S$, $\Omega^\infty = 0$ and $\Omega^\infty = 0{\cdot}9S$ respectively. The curves show the mean velocity minus the linear term $x_2 S$.

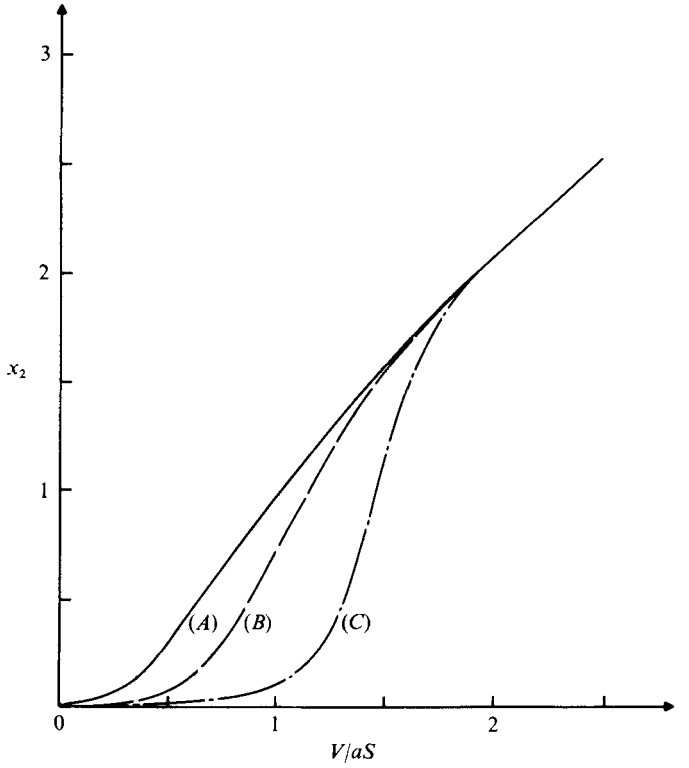

FIGURE 6. Mean particle velocity for (*A*) a suspension of neutrally buoyant couple-free particles ($\Omega = -\frac{1}{2}S$ as $x_2 \to \infty$), (*B*) a suspension of particles subject to an external couple such that $\Omega = 0$ as $x_2 \to \infty$ and (*C*) a suspension of particles subject to an external couple such that $\Omega = 0{\cdot}9S$ as $x_2 \to \infty$. Note that a uniform mean particle distribution is assumed, i.e. (5.1*a*).

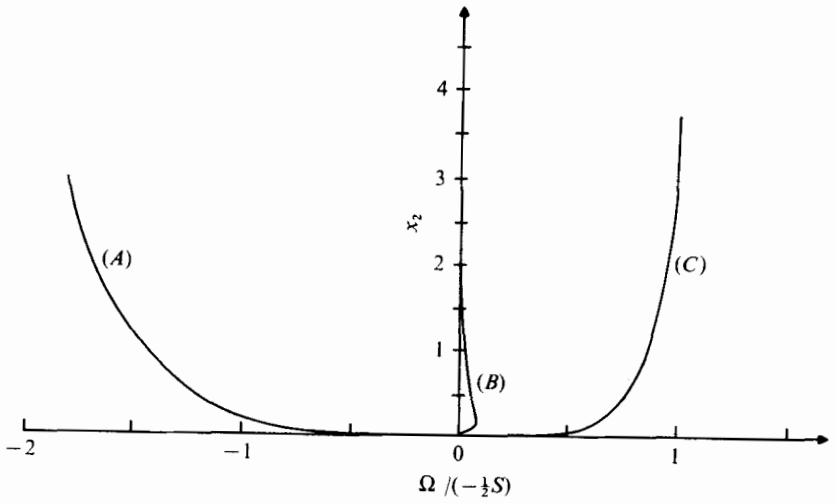

FIGURE 7. Mean particle rotation. Curves (*A*), (*B*) and (*C*) correspond to three different moments applied to the particles giving $\Omega^{\infty} = 0{\cdot}9S$, 0 and $-\frac{1}{2}S$ respectively.

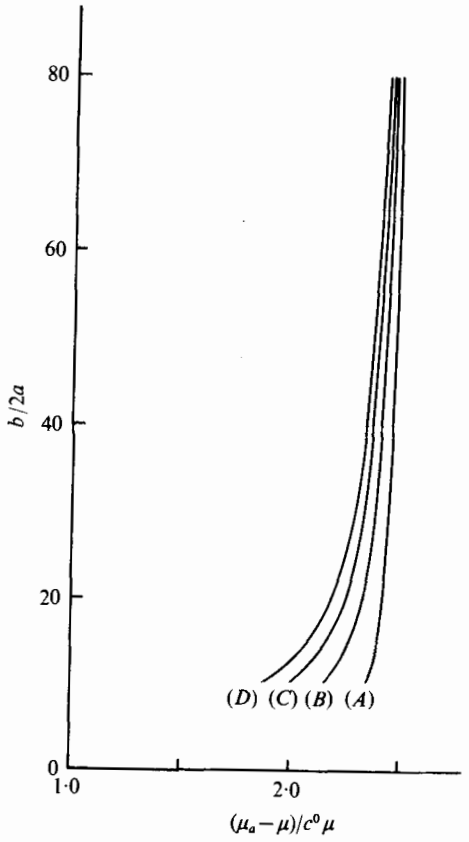

FIGURE 8. Intrinsic apparent viscosity $(\mu_a-\mu)/c^0\mu$ for Couette flow of suspensions of force-free and couple-free particles. Curves (*A*)–(*D*) correspond to particle distribution curves (*a*)–(*d*) of figure 3 respectively.

the mean particle rotation computed over the same area A^* is shown in figure 7. Here the retardation due to the boundary is evident.

It should be noted that the inhomogeneities existing near the walls do not affect the bulk rheological properties of the suspension far from the wall, but rather the wall layer governs the boundary conditions that are to be imposed on the dependent macroscopic variables of the bulk suspension. For specific geometric boundaries, the gross results of the interplay of the bulk suspension and the boundary conditions imposed by the wall layer may be conveniently summarized in terms of an 'apparent viscosity'.

The apparent viscosity for a finite Couette flow between two plates at a distance b apart was computed using (4.11) (for the same applied moments as before). The results for μ_a as a function of $b/2a$ are shown in figure 8. It can be seen that, owing to the wall exclusion effect, the apparent viscosity is noticeably reduced when b/a is less than 40. This reduction is relative to the effective viscosity of an infinite fluid with the concentration c^0 which occurs far from the wall.

Experimentally, wall effects are not detectable in Couette viscometers for dilute suspensions of neutrally buoyant spheres (Maude & Whitmore 1956). This has been explained on the basis that any exclusion of particles from the wall region must result in an increased concentration elsewhere, the average remaining constant. To test this empirical suggestion, the mean concentration τ corresponding to curves (a)–(d) in figure 3 may be computed from

$$\tau = \frac{1}{b}\int_0^b c(x_2)\,dx_2 \tag{5.3}$$

and the apparent viscosity computed for τ from the Einstein formula

$$\bar{\mu}_e = \mu(1 + 2{\cdot}5\tau). \tag{5.4}$$

If the values for $\bar{\mu}_e$ given by (5.4) are used in place of μ_a and plotted as in figure 8, the resultant curves all agree with the curves shown in figure 8 to within 1 % except for the part of curve (A) below $b/2a < 20$, where the error increases to about 3 %. This shows that the present results agree closely with the experimental observations in this regard.

The present results are in disagreement with one previous theoretical analysis (Guth & Simha 1936) which concluded that the apparent viscosity in Couette flow should always be greater than (5.4) owing to the presence of the walls (see Happel & Brenner 1963, pp. 443–445). This is due to the fact that they assume that the mean Couette velocity profile remains linear and do not take into account its modification in the wall layer.

The present results also disagree in a qualitative way with the predictions of mean velocity profiles for Couette flow of micropolar fluids, which have sometimes been suggested as models of suspensions. For the case of zero external moment, the velocity difference shown in figure 5 (curve A) would be negative for a micropolar fluid (see Cowin 1974). For the actual suspension, the velocity difference (figure 5) is always positive. This implies that a micropolar fluid may not be a satisfactory model in this case. (A more detailed discussion may be found in Tözeren 1974.)

For the case of a suspension flowing in a circular cylindrical tube, the apparent viscosities computed using (4.19) are shown as curves (A)–(D) in figure 8. These

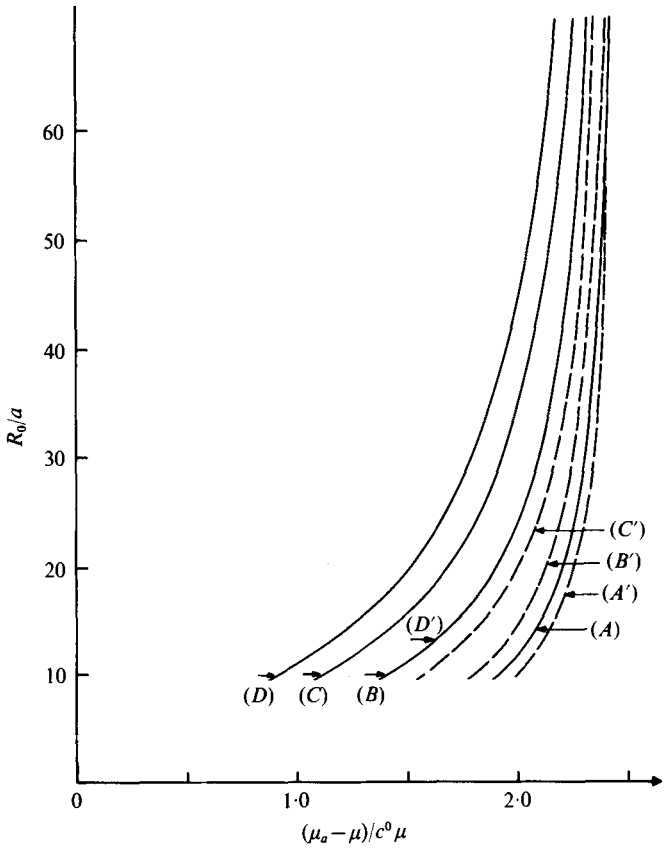

FIGURE 9. Intrinsic apparent viscosity $(\mu_a-\mu)/c^0\mu$ for pipe flow of suspensions of force-free and couple-free particles. Curves (A)–(D) correspond to particle distribution curves (a)–(d) of figure 3 respectively. Curves (A')–(D'), corresponding to curves (a)–(d) of figure 2, were obtained using (5.3).

results are generally lower than those for Couette flow. It is well known experimentally that the apparent viscosity of suspensions decreases with decreasing radius of the tube if the particle size is held fixed (Maude & Whitmore 1956; Whitmore 1959; Seshadri & Sutera 1970). This trend is found also in the flow of blood in capillaries, where it is known as the Fahraeus–Lindquist effect (see Barbee & Cokelet 1971). In all cases it is associated with axial concentration of the suspended particles, due to wall exclusion and radial migration. In the case of blood flow Barbee & Cokelet (1971) show that the experimental results correspond to the apparent viscosity of a uniform particle concentration equal to the spatial average of the concentration in the capillary. For the case of dilute suspensions of rigid spheres treated here, this rule would give again the Einstein infinite-suspension result using the mean concentration $\bar{c}$ in place of c_0. The apparent viscosity would be estimated as

$$\bar{\mu}_e = \mu(1+2{\cdot}5\bar{c}) = \mu\left(1+\frac{5}{R_0^2}\int_0^{R_0} rc(r)\,dr\right). \tag{5.5}$$

Curves (A')–(D') in figure 9 show results computed using (5.5) and the assumed concentration curves (a)–(d) in figure 3. These results show that there is a further

reduction in the apparent viscosity computed by the full theory presented above (curves A–D) as compared with the results obtained using (5.5) (curves A'–D'). This may be attributed to the enhanced role of the reduced particle concentration near the wall, where the velocity gradient is greatest and hence amplifies the effect of this region.

The present results (figure 9, curves A' and B') bridge the experimental data and semi-empirical theory given by Maude (1967) for moderately dilute suspensions of neutrally buoyant spheres ($0{\cdot}07 \leqslant c^0 \leqslant 0{\cdot}20$). This implies that for tube flow the resultant concentration profile near the wall lies between curves (a) and (b) in figure 3(B). Maude (1967) uses curve (a) of figure 3(B) but makes the rough approximation for the wall layer that it consists of only suspending fluid for $0 < x_2 < 1$.

The results of the present analysis can be closely approximated for the case of a uniform distribution of sphere centres (curve (a) in figure 3B) by using a slip velocity at the wall as a boundary condition instead of the usual zero velocity. Using the asymptotes shown in figure 5, the slip velocity at the wall should be

$$U_w = aS_0 c^0[3 + 3{\cdot}3\Omega/S + 0{\cdot}412\,(\Omega/S_0)^2], \tag{5.6}$$

where S_0 is the velocity gradient in the bulk flow approaching the wall but outside the wall layer, and Ω/S is the constant ratio of the particle angular velocity to the mean velocity gradient far from the wall determined by (4.6) and (4.7). Using (5.6) as a boundary condition and assuming a uniform apparent viscosity equal to its value far from the wall will give good approximation of the mean velocity profile far from the wall and down to within about one particle diameter from the wall.

The authors take pleasure in thanking Professor Shu Chien and Professor Maciej Bieniek for helpful discussions of various parts of the subject. The research was made possible by support from the National Heart and Lung Institute through Grants 2R01-HL-13083 and 1-P01-HL-16851.

REFERENCES

ARIMAN, T., TURK, M. A. & SYLVESTER, N. D. 1973 Microcontinuum fluid mechanics – a review. *Int. J. Engng Sci.* **11**, 905–930.

ARIMAN, T., TURK, M. A. & SYLVESTER, N. D. 1974 Applications of microcontinuum fluid mechanics. *Int. J. Engng Sci.* **12**, 279–293.

BARBEE, J. H. & COKELET, G. R. 1971 The Fahraeus effect. *Microvasc. Res.* **3**, 6–21.

BATCHELOR, G. K. 1970 The stress system in a suspension of force-free particles. *J. Fluid Mech.* **41**, 545–570.

BATCHELOR, G. K. 1971 The stress generated in a non-dilute suspension of elongated particles by pure straining motion. *J. Fluid Mech.* **46**, 813–829.

BATCHELOR, G. K. 1973 Transport properties of two-phase materials with random structure. *Lecture at 4th Can. Nat. Cong. Appl. Mech. Univ. Toronto.*

BATCHELOR, G. K. & GREEN, J. T. 1972 The determination of the bulk stress in a suspension of spherical particles to order c^2. *J. Fluid Mech.* **56**, 401–427.

BRENNER, H. 1972*a* Suspension rheology. *Prog. Heat Mass Transfer* **5**, 89–129.

BRENNER, H. 1972*b* Dynamics of neutrally buoyant particles in low Reynolds number flows. *Prog. Heat Mass Transfer* **6**, 509–574.

BRENNER, H. & WEISSMAN, M. H. 1972 Rheology of a dilute suspension of di-polar spherical particles in an external field. II. Effect of rotary Brownian motion. *J. Colloid Interface Sci.* **41**, 499–531.

BUNGAY, P. M. & BRENNER, H. 1969 Modeling of blood flow in the microcirculation-tube flow of rigid particle suspension. *Proc. 7th Ann. SES meeting. St. Louis, Missouri.*

BUNGAY, P. M. & BRENNER, H. 1973 Pressure drop due to the motion of a sphere near the wall bounding a Poiseuille flow. *J. Fluid Mech.* **60**, 81–96.

COWIN, S. C. 1974 The theory of polar fluids. *Adv. in Appl. Mech.* **14**, 295–368.

COX, R. G. & BRENNER, H. 1971 The rheology of a suspension of particles in a Newtonian fluid. *Chem. Engng Sci.* **26**, 65–93.

DEAN, W. R. & O'NEILL, M. E. 1963 A slow motion of viscous liquid caused by the rotation of a solid sphere. *Mathematika* **10**, 13–24.

EINSTEIN, A. 1906 Eine neue Bestimmung der Molekuldimensionen. *Ann. Phys.* **19**, 289–306.

GOLDMAN, A. J., COX, R. G. & BRENNER, H. 1967 Slow viscous motion of a sphere parallel to a plane wall – I, II. *Chem. Engng Sci.* **22**, 637–660.

GUTH, E. & SIMHA, R. 1936 Über die Viskostat von Kugelsuspensionen. *Kolloid Z.* **74**, 266–275.

HAPPEL, J. & BRENNER, H. 1973 *Low Reynolds Number Hydrodynamics*, 2nd edn. Noordhoff.

HINCH, E. J. 1972 Note on the symmetries of certain material tensors for a particle in Stokes flow. *J. Fluid Mech.* **54**, 423–425.

HINCH, E. J. & LEAL, L. G. 1972 The effects of Brownian motion on the rheological properties of a suspension of non-spherical particles. *J. Fluid Mech.* **52**, 683–712.

JEFFERY, G. B. 1915 *Proc. Lond. Math. Soc.* **14**, 327–338.

LEAL, L. G. & HINCH, E. J. 1972 The effect of weak Brownian rotations on particles in shear flow. *J. Fluid Mech.* **55**, 745–765.

MAUDE, A. D. 1967 Theory of wall effect in the viscometry of suspensions. *Brit. J. Appl. Phys.* **18**, 1193–1197.

MAUDE, A. D. & WHITMORE, R. L. 1956 Wall effect and viscometry of suspensions. *Brit. J. Appl. Phys.* **7**, 98–102.

O'NEILL, M. E. 1964 A slow motion of viscous liquid caused by a slowly moving sphere. *Mathematika* **11**, 67–74.

O'NEILL, M. E. 1968 A sphere in contact with a plane wall in a slow linear shear flow. *Chem. Engng Sci.* **23**, 1293–1298.

ROSCOE, R. 1967 On the rheology of a suspension of viscoelastic spheres in a viscous liquid. *J. Fluid Mech.* **28**, 273–293.

SESHADRI, V. & SUTERA, S. P. 1970 Apparent viscosity of coarse, concentrated suspensions in tube flow. *Trans. Soc. Rheol.* **14**, 351–373.

TÖZEREN, A. 1974 Stress in a suspension near rigid boundaries. Ph.D. dissertation, Columbia University, New York.

WHITMORE, R. L. 1959 The viscous flow of disperse suspensions in tubes. In *Rheology of Disperse Systems* (ed. C. C. Mills), pp. 45–56. Pergamon.